International Journal of Science and Research Archive
eISSN: 2582-8185
Cross Ref DOI: 10.30574/ijsra
Journal homepage: https://ijsra.net/

(RESEARCH ARTICLE)

NANOSCALE INVESTIGATION OF LOCAL ELECTRICAL PROPERTIES AND SCHOTTKY CONTACTS IN ALUMINUM-DOPED ZINC OXIDE THIN FILMS USING CONDUCTIVE ATOMIC FORCE MICROSCOPY

Jamal Shaibo [1, 2, *]

[1] Centre for Quantum Materials and Technologies (CQMT), School of Mathematics and Physics, Queen's University Belfast, Belfast BT7 1NN, UK.
[2] Department of Physics, Faulty of Science, University of Nyala, Nyala, 63311, Sudan.
* Corresponding Author

ORCID Details
Jamal Shaibo: https://orcid.org/0009-0002-3896-0907

International Journal of Science and Research Archive, 2026, 20(03), 122–127

Publication history: Received on 24 July 2026; revised on 02 September 2026; accepted on 04 September 2026

Article DOI: https://doi.org/10.30574/ijsra.2026.20.3.1723

ABSTRACT

Aluminum-doped zinc oxide (AZO) thin films were deposited on silicon substrates using radio-frequency (RF) reactive magnetron sputtering. Conductive atomic force microscopy (C-AFM) was used to analyze the surface morphology and local electrical properties of the films. The results show a uniform surface morphology with a grain size of 50 to 100 nm and a surface roughness of approximately 8 nm. C-AFM current mapping reveals a non-uniform current distribution, where electrical current is localized on the grain surfaces and absent at the grain boundaries. Local current-voltage (I-V) curve measurements indicate that the conductive tip forms a Schottky contact (a metal-semiconductor barrier with rectifying properties) with the film, with starting voltages varying by location. Fitting the I-V curves yields the specific ideality factors (parameters measuring how closely a diode follows ideal thermionic emission theory) of the local Schottky barriers.

Keywords: AZO, Reactive Magnetron Sputtering, C-AFM, Schottky Contact, Microscopic Electrical Properties

1 INTRODUCTION

Zinc oxide (ZnO) is a key material in the family of wide-bandgap semiconductors [1]. It has a hexagonal wurtzite crystal structure [1]. Its room-temperature bandgap is 3.37 eV. Its exciton binding energy is 60 meV [1,2]. (An exciton is a bound state of an electron and an electron hole). Researchers study ZnO because it works well in surface acoustic wave devices, ultraviolet detectors, and transparent electronics [1-3]. Scientists improve ZnO electrical properties by adding different types and amounts of dopants. Aluminum-doped zinc oxide (AZO) is a top choice for transparent conductive materials [3,4]. AZO films have high visible-light transparency and good electrical conductivity at room temperature [3].

Most past studies focus on how fabrication methods and substrates change the optoelectronic and structural properties of AZO films [5-10]. Other studies look at post-treatment methods, such as high-temperature annealing and plasma

treatments [11,12]. However, few studies look at the microscopic electrical properties of AZO films. Macroscopic tests measure large areas all at once. These large-scale tests hide important details at the nanoscale level. They cannot show how electricity moves through individual crystal grains or grain boundaries (the edges where grains meet). Grain boundaries often trap electrons. They can create barriers that slow down electrical current. Standard testing tools cannot measure these small electrical behaviors.

This study uses advanced nanoscale tools to examine AZO films. We deposited AZO thin films on silicon substrates using radio-frequency (RF) reactive magnetron sputtering. We used conductive atomic force microscopy (C-AFM) to study the surface shape and local electrical currents at the same time. C-AFM current mapping helps us see where electricity flows on individual grains. We also measured local current-voltage (I-V) curves to understand the Schottky contacts (metal-semiconductor barriers with rectifying properties) formed by the conductive tip. This work reveals the exact origins of non-uniform current distribution in AZO films.

2 EXPERIMENTAL METHOD

2.1 Sample Preparation

The AZO films were prepared using an RF reactive magnetron sputtering system (model JGP450). A Zn-Al alloy target (60 mm in diameter and 3 mm thick, with an Al mass fraction of 3%) was used as the sputtering source. (100)-oriented Si substrates (10 mm × 10 mm) were employed. Prior to sputtering, the Si substrates underwent a cleaning process: ultrasonic cleaning for 5 minutes each in acetone, ethanol, and deionized water; immersion for approximately 20 hours in a mixture of H_2SO_4 and H_3PO_4 (3:1 volume ratio) to remove surface oil and other contaminants; rinsing with deionized water followed by etching in 5% HF solution for 2 minutes to remove the native oxide layer; and finally, thorough rinsing with deionized water, drying with high-purity nitrogen gas, mounting onto a sample holder, and rapid insertion of the holder into the vacuum chamber. During deposition, the substrate-to-target distance was set to 60 mm, and the deposition temperature was maintained at room temperature. A mixture of Ar and O_2 gases was used, with the O_2 volume fraction set at 5% and the flow rate controlled at 30 sccm, working pressure of 0.7 Pa, RF input power to the sputtering target of 120 W, and deposition time of 1 h.

2.2 Sample Characterization

Analysis of the AZO thin film's surface morphology, along with the acquisition of corresponding current maps and localized I-V curves, was performed using a Benyuan CSPM5000 probe microscope in Conductive Atomic Force Microscopy (C-AFM) mode. Scanning areas of 500 nm × 500 nm and 200 nm × 200 nm were selected. With a reference voltage of 0.3 V, the contact force between the probe tip and the thin film sample was calculated to be 8.92 nN based on the force-distance curve.

3 RESULTS AND DISCUSSION

Morphology and current mapping of the sample were conducted using the C-AFM mode of an atomic force microscope. Figure 1 presents the morphology image and the corresponding current map of the AZO thin film sample obtained at a bias voltage of 0.1 V. The morphology image reveals a relatively uniform surface with grain sizes ranging from 50 to 100 nm and a surface roughness of 6.64 nm. The current map on the right shows that, at a bias of 0.1 V, distinct current signals appear in localized regions of the film surface, though the conductive areas are not uniformly distributed. A comparison between the morphology and the corresponding current map indicates that high current values are concentrated on the grains; this suggests that, at the applied bias, most grains are in a conductive state, whereas the grain boundaries are non-conductive.

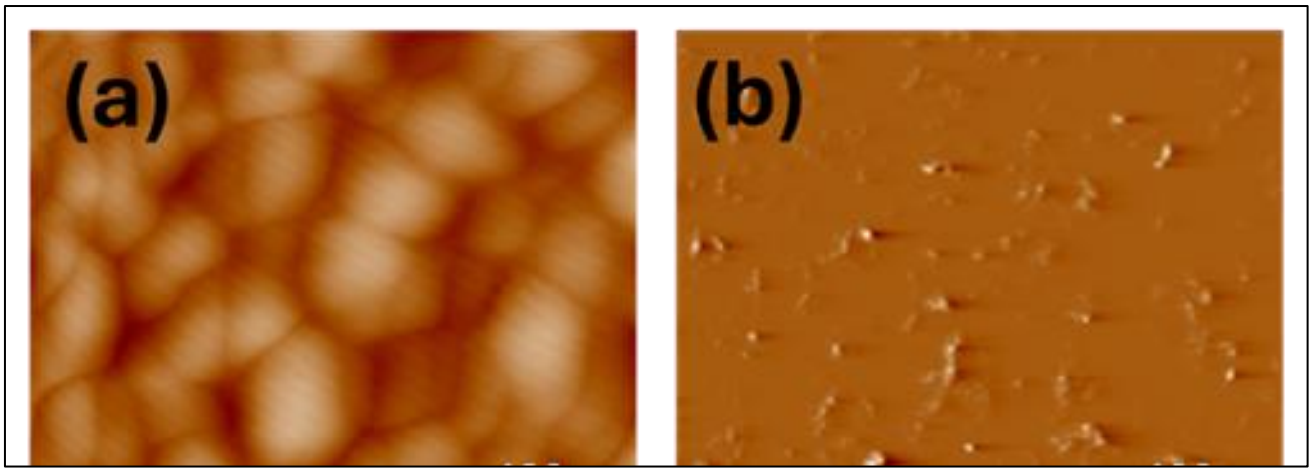

Figure 1: (a) Surface morphology of AZO film samples and (b) corresponding current images obtained at a bias voltage of 0.1 V.

Figure 2 shows C-AFM images obtained at different bias voltages. As can be seen from the figure, the measured current images differ significantly depending on the bias voltage applied to the sample. As the magnitude of the bias voltage increases, the conductive regions expand, and the conduction current rises. We observed that the current images depend not only on the magnitude of the applied bias but also on its polarity. Figures 2(a) and 2(c) show current images of the same location acquired at bias voltages of +0.1 V and -0.1 V, respectively. It is evident that upon the application of a negative bias, the current intensity on the sample surface increases markedly, and the conductive regions expand.

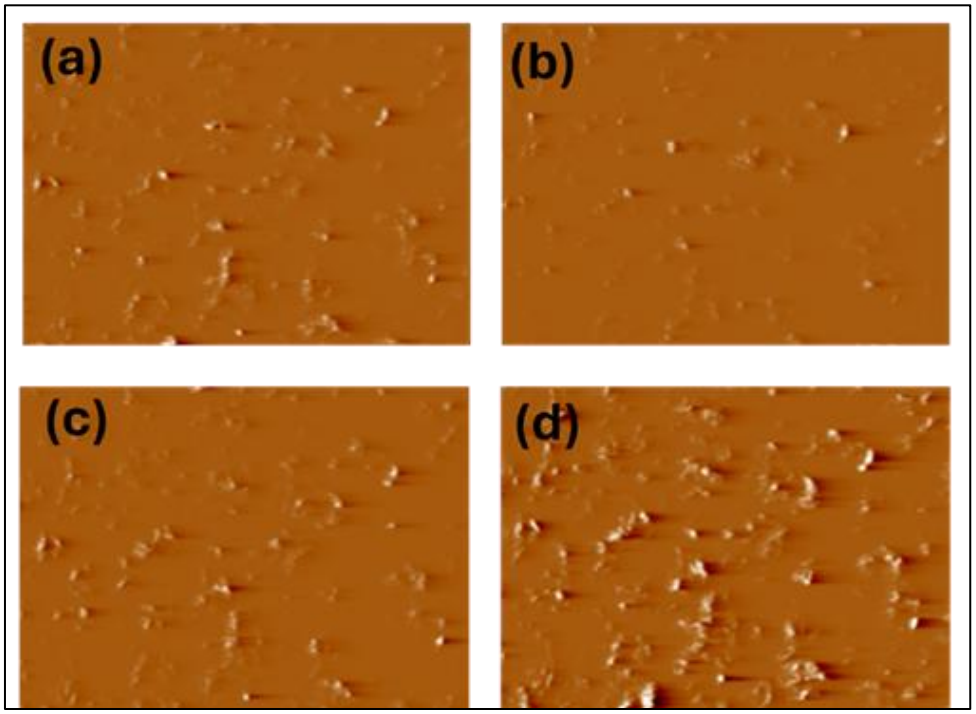

Figure 2: Local current maps of AZO thin films at various bias voltages: (a) 0.1 V, (b) 0.05 V, (c) -0.05 V, and (d) -0.1 V.

To more clearly identify the locations of the conductive regions, we superimposed the topographic image and the corresponding current map for analysis, as shown in Figure 3. Figure 3(c) clearly reveals that the current is primarily localized on the grains, whereas virtually no current is observed at the grain boundaries. To further investigate this phenomenon, we performed localized I-V curve measurements on the sample.

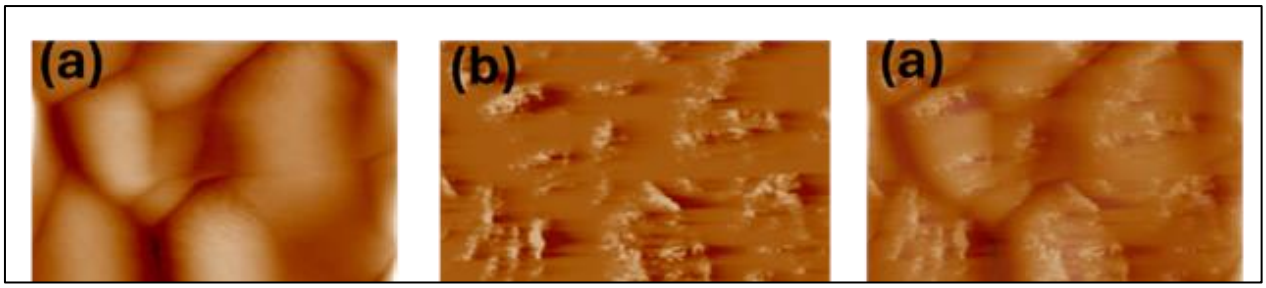

Figure 3: The topography image (a) and current image (bias voltage of 0.1 V)(b) of the AZO film sample and the superposition graph of the morphology and the current image (c.

Figure 4 shows the I-V curves and corresponding morphology images for three distinct points on the AZO thin film, with the bias voltage swept between -0.1 V and 0.1 V. Points A, B, and C in the morphology images correspond to a small grain, a grain boundary, and a large grain, respectively. It can be observed that the turn-on voltages for points A, B, and C are approximately -0.23 V, -0.48 V, and -0.08 V, respectively; this indicates that current flows preferentially in regions located on the grains, whereas regions at the grain boundaries require a higher bias voltage for current to flow. Regarding this phenomenon, some studies attribute it to the presence of numerous defects-such as screw dislocations-at the grain boundaries that impede electron transport, while the grains themselves contain fewer defects, thereby facilitating electron transport more effectively than the grain boundaries [13-15]. While this explanation accounts for the structural characteristics of the thin film, it overlooks the physical mechanism of the Schottky barrier; to further investigate the underlying mechanism of this phenomenon, we performed data fitting on the measured I-V curves. Based on thermionic emission theory, the current-voltage relationship of a Schottky barrier can be described by the following equation [16,17]:

$$I = I_s(\exp\left(\frac{qV}{nk_BT}\right))$$

Here, I is the total current, the saturation current is given by $I_s = AA^*T^2\exp\left(-\frac{q\phi_b}{k_BT}\right)$, where A* is the effective Richardson constant, n is the ideality factor, A is the contact area between the probe and the sample, ϕ_b is Schottky barrier height, q is the elementary charge, k_B is the Boltzmann constant, and T is the test temperature. When qV > 3kT, the current-voltage relationship approximates to $\ln I = \ln Is + qV/nk_BT$; the plot of ln I versus V should be a straight line, from the slope of which the ideality factor n can be determined, while ln Is can be obtained from the intercept on the vertical axis. In this manner, we obtained the ideality factor n for the three I-V curves.

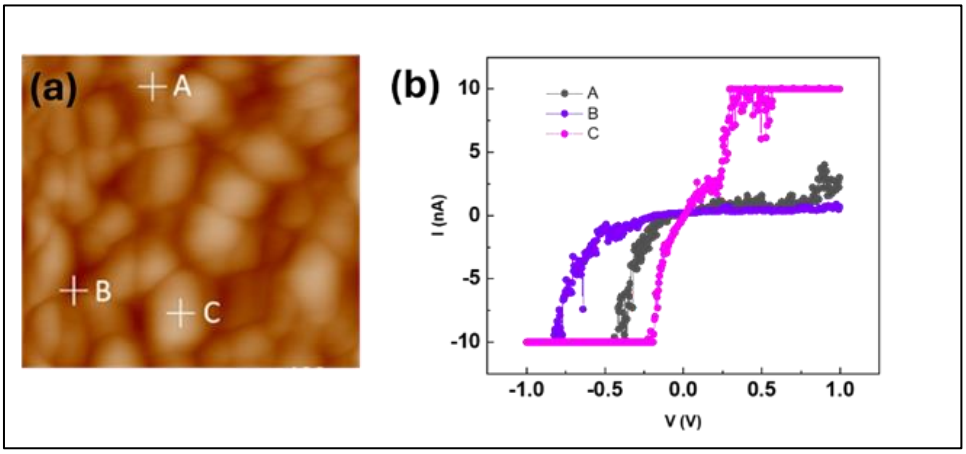

Figure 4: Current-voltage (I-V) characteristics of the AZO thin film samples measured at three different locations (A, B, and C).

Figure 5 presents the fitting results of the I-V curves obtained at three points on the AZO thin film. Linear fitting of the I-V curves yielded ideality factors of 3.66, 6.52, and 2.62 for points A, B, and C, respectively. Point C, which exhibits the lowest ideality factor, is located atop a large grain and is the site where current first appears; conversely, point B, with the highest ideality factor, is situated at a grain boundary and requires a higher bias voltage for current to flow. This indicates that the magnitude of the ideality factor reflects the physical properties of the Schottky junction. To further understand this phenomenon, it is necessary to analyze the Schottky junction formed at the contact interface between the probe tip and the thin-film grain.

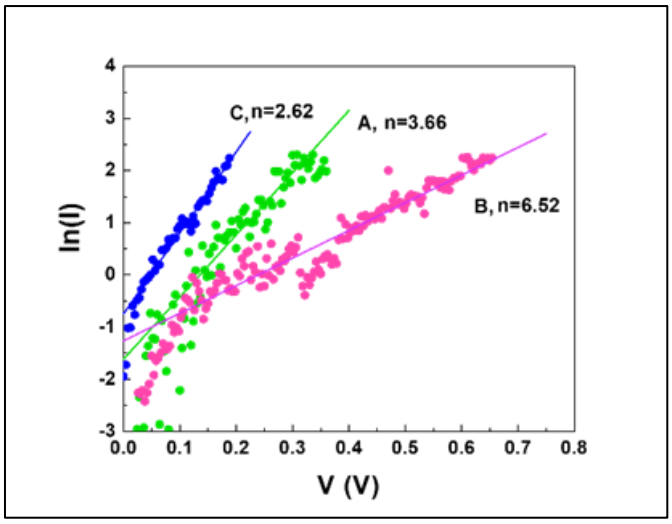

Figure 5: Linear fitting of the I-V curves at points A, B, and C, and the corresponding ideal factors of the Schottky barrier.

During C-AFM measurements, a Schottky contact is formed between the platinum-coated tip and the AZO thin film. The tip diameter is approximately 40 nm a scale comparable to the sample's grain size meaning the contact area directly determines the cross-sectional area of the resulting Schottky junction. Although a constant contact force is maintained during measurement, the tip-sample contact area varies with position due to the surface's inherent roughness; consequently, the area of the Schottky junction also varies. When the tip contacts a grain boundary, the contact area is larger, causing the Schottky junction to deviate significantly from ideal behavior and resulting in a higher ideality factor. Conversely, when the tip contacts a grain, the contact area is relatively small, and the junction behaves more ideally, yielding a lower ideality factor. Therefore, we conclude that the C-AFM current images are significantly influenced by the thin film's morphology.

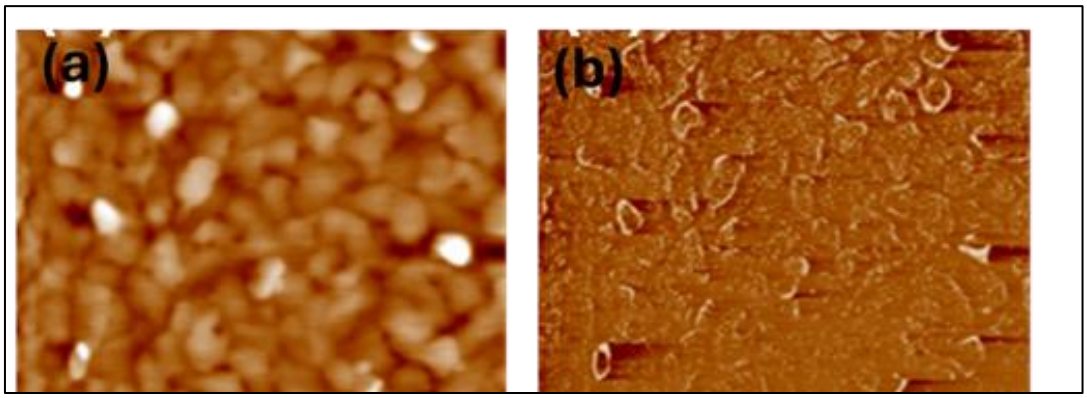

Figure 6: (a) Morphology of platinum film samples and (b) their corresponding current images obtained at a bias voltage of -0.1 V.

To confirm our hypothesis, we performed C-AFM measurements on the Pt metal thin film, as shown in Figure 6. The figure shows a Pt metal thin film grown on a sapphire substrate using reactive magnetron sputtering. The C-AFM image clearly shows that the current appears primarily at the grain locations, while no current is observed at the grain boundaries. Furthermore, the grain shape is clearly visible in the current image. This means that for a metal thin film with good conductivity, the presence or absence of current during C-AFM testing is often influenced by the shape effect of the morphology.

4 CONCLUSION

C-AFM results indicate that the non-uniform current distribution observed in AZO thin films is related to the geometric dimensions and shape of the AFM probe tip. This non-uniformity arises from variations in the Schottky barrier caused by the interplay between the tip geometry and the film's surface morphology; it is not directly linked to factors such as dislocation density or compositional segregation within the film itself. C-AFM results for Pt thin films demonstrate that non-uniform current distribution driven by surface morphology effects occurs in metal thin films as well. Consequently,

whether analyzing metal or semiconductor thin films via C-AFM, the current distribution is influenced by the morphological interaction between the probe tip and the film surface, preventing a true reflection of the sample's intrinsic microscopic electrical properties.

STATEMENTS ON COMPLIANCE WITH ETHICAL STANDARDS

Acknowledgments

The author thanks our colleagues at School of Mathematics and Physics and mentors for their valuable guidance and support throughout the study.

Funding Source

This study was supported through the assistance of the School of Mathematics and Physics. Additional support was provided by the Centre for Quantum Materials and Technologies (CQMT), which facilitated access to research facilities. No external commercial funding was received, and the author declared that the funding body had no role in the design, data collection, analysis, or publication of this research.

Disclosure of conflict of interest

The authors declare that they have no conflict of interest.

Author contributions

Conceptualization, methodology, investigation, data curation, formal analysis, visualization, and writing – original draft preparation, writing – review and editing.

Data and Materials Availability

Data are complete and can be freely provided on request by the corresponding author

REFERENCES

[1] Özgür Ü, Alivov YI, Liu C, Teke A, Reshchikov MA, Doğan S, Avrutin V, Cho SJ, Morkoç H A, comprehensive review of ZnO materials and devices. Journal of Applied Physics. 2005; 98(4), 041301.

[2] Look DC, Recent advances in ZnO materials and devices. Materials Science and Engineering: B. 2001; 80(1-3), 383-387.

[3] Kim H, Horwitz JS, Kim WH, Makinen AJ, Kafafi Z H, Chrisey DB. Transparent conducting aluminum-doped zinc oxide thin films for organic light-emitting devices. Applied Physics Letters. 2000; 76(3), 259-261.

[4] Minami T. Transparent conducting oxide semiconductors for electronics with transparent displays. Semiconductor Science and Technology. 2005; 20(4), S35-S44.

[5] Chun AT, Jing CL, Yu FC, San DC, Kun CP. Applied Surface Science. 2012; 258 5996-6002

[6] Jeong SH, Kho S, Jung D, Lee SB, Boo JH. Surface and Coatings Technology. 2003; 174 -175 , 187-192

[7] Kun HK, Ki CP, Dae YM. J. Appl. Phys. 1997; 81 7764

[8] Li C, Furuta M, Matsuda T, Hiramatsu T, Furuta H, Hirao T. Thin Solid Films. 2009; 517 3265-3268

[9] Yaodong L, Jianshe L. Applied Surface Science. 2007; 253 3727-3730

[10] Jaehyeong L, Dongjin L, Donggun L, Keajoon Y. Thin Solid Films. 2007; 515 6094-6098

[11] Shou YK, Wei CC, Fang IL, Chin PC, Hao CK, Shing CW, Wen FH. Journal of Crystal Growth. 2006; 287 78-84

[12] Fang HW, Hung PC, Chih CT, Chia H. Surface & Coatings Techology. 2011; 205 5265-5277

[13] Liu WR, Hsieh WF, Hsu CH, Liang KS, Chien FS. Journal of Crystal Growth. 2006; 297 294-299

[14] Mosbacker HL, Zgrabik C, Hetzer MJ. Applied Physics Letters. 2007; 91 072102

[15] Brillson LJ, Mosbacker HL, Hetzer MJ. 2007; Applied Physics Letters 90 102116

[16] I. Beinik M, Kratzer A, Wachauer L. Wang. J. Appl. Phys. 2011; 110, 052005

[17] Wen G, Ya Y, Jing LYZ. Phys. Chem. Chem. Phys. 2010; 12, 14868-14872